A Minimum Drives Automatic Target Definition Procedure for Multi-Axis Random Control Testing

Umberto Musella[†,a,b,c], Giacomo D'Elia[d], Alex Carrella[b], Bart Peeters[b], Emiliano Mucchi[d], Francesco Marulo[c], Patrick Guillaume[a]

[a] *Vrije Universiteit Brussel, Pleinlaan 1, 1050 Brussels (Belgium)*
[b] *Siemens Industry Software NV, Interleuvenlaan 68, 3001 Leuven (Belgium)*
[c] *University of Naples "Federico II", via Claudio 21, 80125 Naples (Italy)*
[d] *University of Ferrara, via Saragat 1, 44122 Ferrara (Italy)*
[†] *Corresponding author, e-mail: umberto.musella.ext@siemens.com*

Abstract

Multiple-Input Multiple-Output (MIMO) vibration control tests are able to closely replicate, via shakers excitation, the vibration environment that a structure needs to withstand during its operational life. This feature is fundamental to accurately verify the experienced stress state, and ultimately the fatigue life, of the tested structure.

In case of MIMO random tests, the control target is a full reference Spectral Density Matrix in the frequency band of interest. The diagonal terms are the Power Spectral Densities (PSDs), representative for the acceleration operational levels, and the off-diagonal terms are the Cross Spectral Densities (CSDs). The specifications of random vibration tests are however often given in terms of PSDs only, coming from a legacy of single axis testing. Information about the CSDs is often missing. An accurate definition of the CSD profiles can further enhance the MIMO random testing practice, as these terms influence both the responses and the shaker's voltages (the so-called *drives*). The challenges are linked to the algebraic constraint that the full reference matrix must be positive semi-definite in the entire bandwidth, with no flexibility in modifying the given PSDs.

This paper proposes a newly developed method that automatically provides the full reference matrix without modifying the PSDs, considered as test specifications. The innovative feature is the capability of minimizing the drives required to match the reference PSDs and, at the same time, to guarantee that the obtained full matrix is positive semi-definite. The drives minimization aims on one hand to reach the fixed test specifications without stressing the delicate excitation system; on the other hand it potentially allows to further increase the test levels. So far no general solution has been proposed that combines the drives reduction with a resulting positive semi-definite reference matrix, making the available methodologies sometimes unsuitable in practice. The detailed analytic derivation and implementation steps of the proposed method are followed by real-life testing considering different scenarios.

Keywords: Multi-Axis Environmental Testing, MIMO Control, Random Vibration, Minimum Drives Power, Positive Semi-definite Matrix.

1. Introduction

Vibration control tests are performed to verify that a system and all its sub-components can withstand the vibration environment during the operational life. These tests aim to accurately replicate via controlled shaker excitation the in-service structural response of a unit under test in the main axis of vibration and in all the possible axes where the levels exceed the acceptance thresholds [1]. The simplest way to expose a test article to an excitation in multiple axes is to perform a sequential Single-Input Single-Output (SISO) test: sequentially, the test article is rotated, the test set-up changed and a new test is performed with the required SISO profile as test specification. Practical aspects, linked for instance to the sizes of the article to be tested or to issues in changing multiple times the test set-up [2], can make the execution of these tests challenging or even impossible. However, the most critical aspect of a sequential SISO test is that it poorly represents any real vibration environment and therefore can lead to an unacceptable time to failure overestimation for the unit under test and different failure modes [3]. This has been shown in small-scale

problems, such as printed wiring boards testing (where the inductor are critical components) [4] or thin plates [5], but also in large-scale tests, such as large spacecraft vibration testing as shown in [6]. The only alternative to overcome the sequential single-axis test limitations is to apply a simultaneous multi-axial excitation performing a Multi-Input Multi-Output (MIMO) vibration control test [7], [8], [9].

Even though the benefits of MIMO testing are clear and widely accepted by the environmental engineering community, ever since 1958 (the first documented attempt to simultaneous multi-axial excitation [10]), this practice experienced a very slow growth. Initially this was due to the available technology in terms of excitation mechanisms and computational power for the data acquisition hardware and vibration controllers. The first multi-input control algorithm was developed only twenty years later, in 1978 by David Smallwood from Sandia National Laboratories (as documented in the 1982's publication *A Random Vibration Control System for Testing a Single Test Item with Multiple Inputs* [11]) and coped with the available computational power. Modern MIMO vibration control strategies rely on the work of Underwood [12], whose first patent on the topic is dated 1994 [13]. Just recently, the increased complexity, sizes and cost of the article to be tested increased the concern about replicating as close as possible the environments to be tested [2], [14], [15], [16], [17], [18]. The high degree of expertise needed to perform these tests and decades of single axis controlled excitation built meanwhile a legacy of SISO standards that currently represent the main reference for the environmental test engineers. For these reasons nowadays MIMO vibration control tests are still considered as a *pioneering* testing methodology.

There are different types of MIMO tests (random, sine, time waveform replication), depending on the environment a test article needs to be exposed. For automotive and aerospace systems and subsystems, a random vibration test is required for all the main mechanical and electrical components [19]. This type of test is performed to simulate the response of the unit under test to a broadband random Gaussian vibration environment. Typical scenarios are the road excitation or the response to a diffuse acoustic field [20]. For the SISO case the test specification is a Power Spectral Density (PSD, usually in g^2/Hz) profile that needs to be replicated for a user-defined control channel by exciting the unit under test with a single-axis shaker. In the MIMO case, it is possible to define required test levels for multiple control channels that will be controlled simultaneously. Additional information about the cross-correlation between the control channels is also included. This information must be provided in terms of Cross Spectral Densities (CSDs) between pairs of control channels defining desired phase and coherence profiles [8], [9], [14]. The definition of these terms is essential to also replicate the cross-correlation that naturally exists between difference responses. These terms are also controlled by modern vibration controllers. For these systems the control target is thus a full reference Spectral Density Matrix (SDM). The target definition process plays already a key role for MIMO random control tests as documented in recent studies [21], [22], [23], [24].

Theoretically, a successful MIMO random control test can be performed in case the operational environment is fully replicated in the laboratory, meaning that

1. the nature of the operational loads can be exactly replicated with the available exciter(s);
2. the boundary conditions can be also exactly replicated with the available fixtures;
3. operational measurements are available for all the control points.

In the last years significant works have been published that focus on the excitation and boundary conditions replication on the test results. The works of Daborn [17] and [25] on aerodynamically excited structures show how increasing the number of control channels and trying to match the operational impedance, on top of a successful random test, also allows to closely match the response in location that are not controlled. These observations are at the basis of the so-called *IMMAT (Impedance-Matched Multi-Axial Test)* approach [26]. Roberts in [18] shows that the (known) environmental replication further improves by increasing the number of shakers and adopting rectangular control strategies. The approaches require fully available operational measurements. As pointed out in [2], unfortunately operational measurements are not always available and often the test specifications are provided just in terms of PSDs at the control locations. This is due to several reasons. First of all, the gradual transition from sequential SISO testing to simultaneous multi-axial testing needs to face the aforementioned legacy of SISO standards and specifications, provided in terms of PSDs. Second, the standardization of the CSD terms is impractical to implement in a specification due to a lack of knowledge that makes challenging (and even impossibile) to average, smooth or envelope coherence and phase information from different operational conditions. In this case, the choice of setting appropriate values to

fill in the full reference matrix *must reflect the desires of a knowledgeable environmental test engineer* [2]. Defining the reference matrix with no a-priori knowledge of the cross-correlation between control channels is very challenging. Filling in the off-diagonal terms, in fact, must guarantee that the reference matrix will have in the end a physical meaning (realizable). This is translated in the algebraic constraint that this matrix needs to be positive semi-definite and at the same time the test needs to guarantee the required PSDs at the control locations.

The solution of finding a full reference matrix with fixed PSD terms is not unique. These considerations reflect the need of having a method rather than standardized values to define the specification of a multi-axial test.

The objective of this work is to provide a fully automated method to define the MIMO random reference matrix in case of missing operational measurements and the test specifications are provided in terms of (SISO) PSDs only. The full reference matrix returned by the method needs to be positive semi-definite in order to be used for actual testing and ensure good narrowband control performances on the provided PSDs.

In [2] and [29] a solution to the aforementioned problems has been shown to be directly linked to the solution of the so-called problem of *meeting the minimum drives criteria*. In [29] the author proposes the so-called Extreme Input/Output method. The idea behind the method is to find the CSDs that minimize the input power required to reach the (specified) PSDs. Minimizing the input power is directly linked to an excitation that copes with the system's dynamics and therefore the subsequent natural motion obtained by setting the target is also linked to good control performances. Unfortunately, this target definition procedure is not able to guarantee that the final target will be positive semi-definite. This makes the method not suitable for practical testing, as will be shown in the section 3 and Appendix A.

At the authors' knowledge and as highlighted in standards for multi-axial testing *although an active area of research, general techniques to address minimum drives criteria have not been formally estabilished at the time of* [the] *publication* (2014) [2]. It is clear that meeting the minimum drives requirements is still an open bullet in the multi-axial testing community and the fully automated procedure developed in this paper, named *Minimum Drives Method* shows to be an attractive solution. Extending the work of Smallwood [29], the Minimum Drives Method makes use of an accurate phase selection, as introduced in [27] and [28], to overcome the limitation of obtaining positive semi-definite target matrices.

Following this introduction, section 2 briefly summarizes the theoretical background of multi-axial random testing. In section 3 the mathematical formulation and the implementation process of the Minimum (Maximum) Drives Method are explained in details. In section 4, a series of *normal-end* tests will be used to validate the developed procedure, considering different actuation mechanisms, number of drives and control channels. First, the Minimum (Maximum) Drives Method is applied to a simple electronic system. Then, the method is used to define a target for an electrodynamic three-axial shaker and a six-axis servo-hydraulic shaker. With the three-axial excitation, an industrial test case is considered to show how the method can be applied for testing automotive components. The series of tests shows how the developed procedure is able to drastically reduce, with respect to common choices normally used to obtain a positive semi-definite target matrix, the total drives power required to meet the PSD specifications. The single drives will also show drastic power reductions. This enhancement opens the possibility to further increase the test levels (in terms of g_{RMS}) avoiding data acquisition DACs overloads or physical limitations of the excitation systems. With respect to the excitation system, it is also worth to notice that reducing the drive power required to match a target also means to work in safety with the expensive testing equipment.

Since in this work most of the derivations are in the frequency domain, all the arrays are functions of the frequency f (in Hz), if not specified otherwise. Vectors are denoted by lower case bold letters, e.g. $\mathbf{a}$, and matrices by upper case bold letters, e.g. $\mathbf{A}$. An over-bar $\overline{\square}$ is used to indicate the complex conjugate operation and the Hermitian superscript $\square^H$ to indicate the complex conjugate transpose of a matrix, e.g. $\overline{\mathbf{a}}$ and $\mathbf{A}^H$. The dagger symbol $\square^\dagger$ is used to indicate the Moore-Penrose pseudo-inverse of a matrix, whereas the hat $\hat{\square}$ is used to emphasize the estimation of a quantity, e.g. $\hat{\mathbf{A}}$ is an estimate of the matrix $\mathbf{A}$.

2. Theoretical background

Figure 1 shows a general block scheme of a multi-axial random control test. A set of m voltages is sent to the exciters. Typically these signals (the so-called *drives*) drive m independent shakers or the multiple degrees of freedom of a multi-axis exciter. In this case additional kinematic transformations (internal to the data acquisition system or

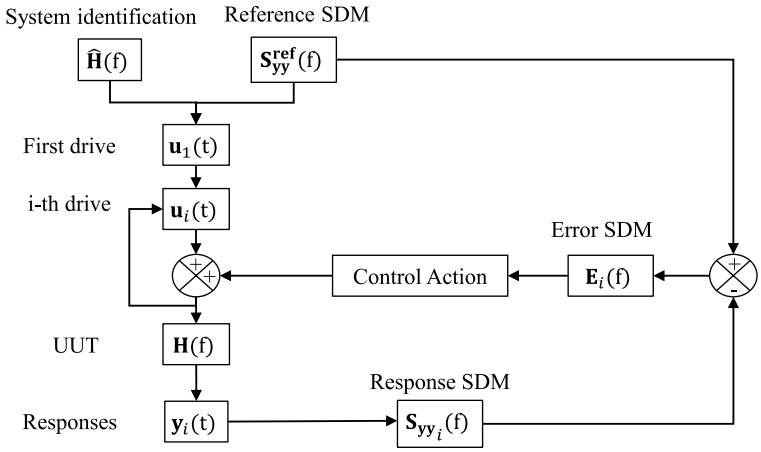

Figure 1: MIMO random control general block scheme.

through an external control logic) translate the voltages in the shaker's motion in the three-dimensional space. The unit under test responses are recorded in ℓ control channels (the so-called *controls* or *pilots*). In case the full dynamic system is linear and time invariant, it is possible to write the Input-Output relation

$$\mathbf{Y} = \mathbf{H}\mathbf{U} \tag{1}$$

where $\mathbf{Y} \in \mathbb{C}^{\ell \times 1}$ and $\mathbf{U} \in \mathbb{C}^{m \times 1}$ are the spectra of the controls $\mathbf{y}(t) = \{y_1(t), \ldots, y_\ell(t)\}^T$ and the drives $\mathbf{u}(t) = \{u_1(t), \ldots, u_m(t)\}^T$, respectively and $\mathbf{H} \in \mathbb{C}^{\ell \times m}$ is the Frequency Response Functions (FRFs) matrix . In all the vibration control tests, a System Identification pre-test phase is always needed to estimate the system's FRFs. This is usually performed by running a low-level random test and using the so called H_1 estimator

$$\hat{\mathbf{H}} = \hat{\mathbf{S}}_{\mathbf{yu}}\hat{\mathbf{S}}_{\mathbf{uu}}^{-1} \tag{2}$$

where $\hat{\mathbf{S}}_{\mathbf{yu}} \in \mathbb{C}^{\ell \times m}$ and $\hat{\mathbf{S}}_{\mathbf{uu}}^{-1} \in \mathbb{C}^{m \times m}$ are spectral density matrices estimated via Welch's averaged periodogram method [31] or other approaches. Once the FRF is known, its inverse can be computed, for example as the Moore-Penrose pseudo-inverse $\mathbf{Z} = \mathbf{H}^\dagger \in \mathbb{C}^{m \times \ell}$, where $\mathbf{Z}$ is often referred as the *System's Impedance Matrix*. Generally a pseudo-inversion is always needed because the number of controls can exceed the number of drives, in what is known in the MIMO control literature as *Rectangular Problem* [7].

In terms of SDMs, it is possible to write the Input-Output relations as

$$\mathbf{S}_{\mathbf{yy}} = \mathbf{H}\mathbf{S}_{\mathbf{uu}}\mathbf{H}^H \tag{3}$$

$$\mathbf{S}_{\mathbf{uu}} = \mathbf{Z}\mathbf{S}_{\mathbf{yy}}\mathbf{Z}^H \tag{4}$$

The objective of MIMO random vibration control tests is to replicate a full SDM $\mathbf{S}_{\mathbf{yy}}^{\mathbf{ref}}$. Theoretically the test target can be directly achieved by sending the input drives that have the specified input spectral density matrix

$$\mathbf{u}(t) = \text{ifft}(\mathbf{U}) : \mathbf{S}_{\mathbf{uu}} \stackrel{\text{def}}{=} E[\mathbf{U}\mathbf{U}^H] = \hat{\mathbf{Z}}\mathbf{S}_{\mathbf{yy}}^{\mathbf{ref}}\hat{\mathbf{Z}}^H \tag{5}$$

with the procedure illustrated in [32]. Nevertheless, due to the possible non-linear behavior of the unit under test and noise in the measurements, the estimated system will inevitably differ from the actual one ($\mathbf{H}\hat{\mathbf{Z}} \neq \mathbf{I}$, where $\mathbf{I}$ is the $\ell \times \ell$ identity matrix)

$$\mathbf{S}_{\mathbf{yy}} = (\mathbf{H}\hat{\mathbf{Z}})\mathbf{S}_{\mathbf{yy}}^{\mathbf{ref}}(\mathbf{H}\hat{\mathbf{Z}})^H \neq \mathbf{S}_{\mathbf{yy}}^{\mathbf{ref}} \tag{6}$$

and a control action is needed to reduce the error

$$\mathbf{E} = \mathbf{S}_{\mathbf{yy}}^{\mathbf{ref}} - \mathbf{S}_{\mathbf{yy}} \tag{7}$$

All the error correction strategies for MIMO random vibration control tests (mainly due to works of Underwood [7],[14], Smallwood [8] and Peeters [9]) rely on the possibility of apply the so called *Cholesky Decomposition* to one of the spectral matrices (either $\mathbf{S}_{\mathbf{yy}}^{\mathbf{ref}}$ or $\mathbf{S}_{\mathbf{uu}}$) and then iteratively correct the resultant *Cholesky Factor*. This operation is perfectly allowed because of the positive semi-definite nature of the spectral density matrices.

In Appendix A it is demonstrated that the SDMs calculated from a set of (random) signals are positive semi-definite. The reference matrix $\mathbf{S}_{\mathbf{yy}}^{\mathbf{ref}}$ set as target of MIMO random control test must then be positive semi-definite to have a physical meaning. The definition and important properties of these matrices are also reported in Appendix A. In case a full set of measurements is not available and test specifications provided in terms of PSD-only breakpoints, the choice of setting the cross-correlation information between pairs of control channels is given to the test engineer. Most of the MIMO vibration controllers give the possibility of defining element-wise the CSDs in terms of (ordinary) coherence and phase profiles [2] (typical values of low coherence and high coherence are $0.01 \div 0.05$ and $0.95 \div 0.98$, respectively). All the CSDs are then easily computed as

$$S_{jk} = |S_{jk}| \exp(\mathrm{i}\phi_{jk}) = \sqrt{\gamma_{jk}^2 S_{jj} S_{kk}} \exp(\mathrm{i}\phi_{jk}) \qquad \forall j,k \quad j \neq k \tag{8}$$

where i is the imaginary unit and j and k are the j-th and the k-th control channels, respectively.

3. Reducing the total drives power in MIMO Random Control Tests

3.1. The state-of-the-art: Extreme Inputs/Outputs Method

The idea of the method proposed in [29] is to find, with fixed PSD levels, the set of coherences and phases between the control channels that minimizes the trace of the drives SDM, i.e.

given $\boxed{diag(\mathbf{S}_{\mathbf{yy}}^{\mathbf{ref}})}$ find $\boxed{\mathbf{S}_{\mathbf{yy}}^{\mathbf{ref}}}$ so that $\boxed{Tr(\mathbf{S}_{\mathbf{uu}} = \mathbf{Z}\mathbf{S}_{\mathbf{yy}}^{\mathbf{ref}}\mathbf{Z}^H)}$ is minimum/maximum

The choice of the drive trace as quantity to be minimized is undoubtedly advantageous because a closed form expression can be derived in terms of the specified PSDs and the unknown coherences and phases between pairs of control channels.

Considering that the general ij-th term in the matrix product $\mathbf{A} = \mathbf{BC}$ (with $\mathbf{A}$ and $\mathbf{B}$ of sizes $m \times p$ and $p \times n$, respectively) can be expressed as $A_{ij} = \sum_k B_{ik} C_{kj}$ and the basic equation (4) for Linear Ttime Invariant (LTI) systems, the diagonal terms of the input SDM can be expressed as

$$S_{uu,ii} = \sum_{j=1}^{\ell} \sum_{k=1}^{\ell} Z_{ik} S_{yy,jk}^{ref} \bar{Z}_{ij} \qquad \forall i = 1:m \tag{9}$$

For the sake of brevity, the superscript $\square^{ref}$ will be dropped in the following derivation. The trace of the drives SDM is the sum of the diagonal terms [30]

$$P \triangleq \mathrm{Tr}(S_{uu}) = \sum_{i=1}^{m} \left(\sum_{j=1}^{\ell} \sum_{k=1}^{\ell} Z_{ik} S_{yy,jk} \bar{Z}_{ij} \right) = \sum_{j=1}^{\ell} \sum_{k=1}^{\ell} S_{yy,jk} \sum_{i=1}^{m} \bar{Z}_{ij} Z_{ik} \tag{10}$$

The single sum on the right-hand-side of equation (10) can be interpreted as the kj-th entry of an hermitian matrix $\mathbf{F} \triangleq \mathbf{Z}^H\mathbf{Z}$. By noticing that $\mathbf{S}_{\mathbf{yy}}^{\mathbf{ref}}$ needs to be hermitian too and that $\mathbf{S}_{\mathbf{uu}}$ inherits the property (see Appendix A), the trace P must be a real number [30] and equation (10) can be rewritten as

$$P = \sum_{j=1}^{\ell} \sum_{k=1}^{\ell} S_{yy,jk} F_{kj} = \sum_{j=1}^{\ell} S_{yy,jj} F_{jj} + 2 \sum_{j=1}^{\ell-1} \sum_{k=j+1}^{\ell} \mathrm{Re}\{S_{yy,jk} \bar{F}_{jk}\} = \sum_{j=1}^{\ell} S_{yy,jj} F_{jj} + 2 \sum_{j=1}^{\ell-1} \sum_{k=j+1}^{\ell} |S_{yy,jk}||F_{jk}| \cos(\phi_{jk} - \theta_{jk}) \tag{11}$$

where $S_{jk} = |S_{jk}| \exp(\mathrm{i}\phi_{jk})$ and $F_{jk} = |F_{jk}| \exp(\mathrm{i}\theta_{jk})$. Equation (11) is explicit in the unknown reference matrix CSD terms. By using the relation (8), equation (11) can be finally expressed in terms of coherences and phases between the pairs of control channels (the information that needs to be provided to the vibration controller)

$$P = \sum_{j=1}^{\ell} S_{yy,jj} F_{jj} + 2 \sum_{j=1}^{\ell-1} \sum_{k=j+1}^{\ell} \sqrt{\gamma_{jk}^2} \sqrt{S_{yy,j} S_{yy,k}} |F_{jk}| \cos(\phi_{jk} - \theta_{jk}) \tag{12}$$

The matrix $\mathbf{F}$ can be easily computed from the identified system $\hat{\mathbf{H}}$, and therefore the terms $|F_{jk}|$ and θ_{jk} can be considered as known quantities. Also the PSD terms are known and considered as test specifications. The first term on the right hand side of equation (12) is always positive and fixed for the given test specifications and test setup. The second term contains the quantities ϕ_{jk} and γ_{jk}^2, unknowns of the target definition procedure. This term can be negative because of the cosine contained in the double sum and can therefore be a negative contribution, reducing the drive trace. The expression in equation (12) has a minimum (maximum) when the coherences are all unitary and the cosines all equal -1 (1). This observation leads to the following conditions (addressed here as *Extreme Drives Conditions*) that lead to the theoretical minimum (maximum) drive traces

$$P \text{ is minimum} \iff \begin{cases} \gamma_{jk}^2 = 1 \\ \phi_{jk} = \theta_{jk} + \pi \end{cases} \qquad \forall\, j,k = 1:\ell,\ j \neq k \tag{13a}$$

$$P \text{ is maximum} \iff \begin{cases} \gamma_{jk}^2 = 1 \\ \phi_{jk} = \theta_{jk} \end{cases} \qquad \forall\, j,k = 1:\ell,\ j \neq k \tag{13b}$$

In the following the conditions (13a) and (13b) will be referred as the *Minimum Drives Condition* and the *Maximum Drives Condition*, respectively. All the other possible combinations of coherences and phases return drive traces that fall in the range between the minimum and the maximum value.

3.2. Minimum (Maximum) Drives Method: phase selection for coherent positive semi-definite reference matrices

Condition (13a) requires to fill in the MIMO reference matrix *element by element* with $\ell(\ell+1)/2 - \ell$ unitary coherence and phase profiles equal to the $\theta + \pi$ phase angle of the $\mathbf{F}$ matrix corresponding entry (the same considerations hold for (13b)). This could result in the reference matrix being negative definite. A mathematical proof can be found by analyzing the simple case of three control channels. Stated that the only physical values that the coherence can assume are between 0 and 1, for the reference matrix to be positive semi-definite it is necessary and sufficient that the Sylvester's Criterion holds (see property (c) in Appendix A) and therefore that

$$det(\mathbf{S}_{\mathbf{yy}}^{\mathbf{ref}}) = 1 - \gamma_{12}^2 - \gamma_{13}^2 - \gamma_{23}^2 + 2\cos(\phi_{12} - \phi_{13} + \phi_{23}) \sqrt{\gamma_{12}^2\, \gamma_{13}^2\, \gamma_{23}^2} \geq 0 \tag{14}$$

Unitary coherence implies also the cosine to be unitary, in order for the determinant to be greater or equal than zero and thus the cosine's argument must nullify

$$\begin{cases} det(\mathbf{S}_{\mathbf{yy}}^{\mathbf{ref}}) \geq 0 \\ \gamma_{12}^2 = \gamma_{13}^2 = \gamma_{23}^2 = 1 \end{cases} \Rightarrow \phi_{12} - \phi_{13} + \phi_{23} = 0 \tag{15}$$

A strong deterministic relation needs to exist between the phases to be selected. This can be physically explained by associating these phases to the ones of the respective recorded spectra, as shown in Figure 2[1]. Setting the phases ϕ_{12} and ϕ_{13} means to set a *relative constraint* in the phase information carried by the two pairs of recorded signals, i.e. that between controls 1 and 2 and controls 2 and 3 there are phase angles (in radians) of ϕ_{12} and ϕ_{13}, respectively. Therefore, the phase ϕ_{23} between the control channels 2 and 3 is unequivocally defined as the difference between ϕ_{13} and ϕ_{12}.

[1] Even though a simple signal processing consideration justifies the realisability of the fully coherent reference matrix obtained with the derived relative phases, an extended mathematical derivation for the general case of ℓ control channels based on the Sylvester's Criterion is unfeasible at the authors' knowledge.

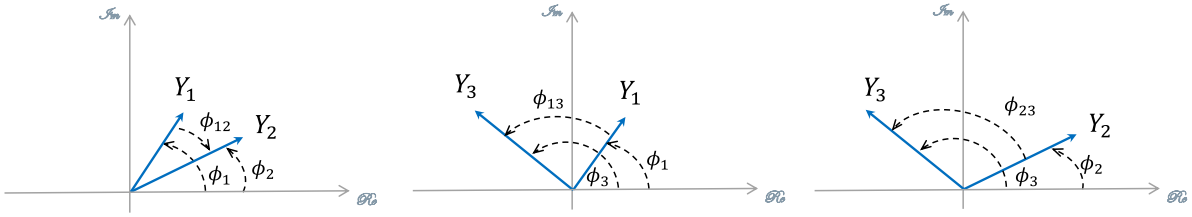

Figure 2: Example of phase relation for three fully coherent control channels. Given the phases ϕ_{12} and ϕ_{13}, the phase ϕ_{23} is unequivocally defined as the difference between the other two.

Keeping unitary coherence, equation (15) highlights that, unless the $\theta + \pi$ angles does not already respect the aforementioned relation, a physical realizable target to be used for testing purposes cannot be set with the conditions (13).

Nevertheless, equation (12) still provides a solution to reduce the drives power. A positive semi-definite matrix can be obtained selecting just $\ell - 1$ phases equal to the respective $\theta + \pi$ phase angles whereas all the others needs to be obtained in order to fulfill the condition (15), i.e. as the difference between the selected ones. This means that an automatic target definition procedure can return positive semi-definite reference matrices and drastically reduce the drives power (without any modification on the PSDs) if these $\ell - 1$ phases are opportunely chosen and the remaining ones calculated in order to agree with this simple principle.

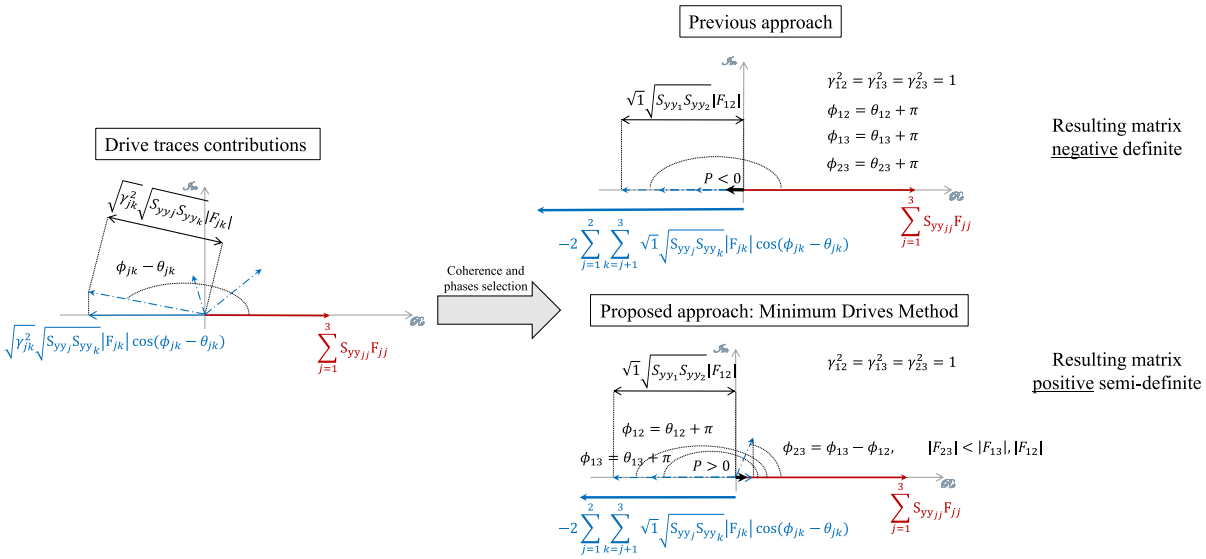

Figure 3: *Minimum Drives Method* principle.

Figure 3 gives a graphical interpretation of equation (12) that can be used to better understand, for the three control case, how to select the best phases. The drive trace can be seen as the summation of two real terms: the single sum in equation (12) is fixed and always positive and is represented by the red solid arrow in Figure 3. The solid blue arrow is representative for the double summation in equation (12). This term is tunable since it contains the phase and the coherence between pairs of control channels that need to be defined. Each contribution to the sum can be interpreted as the projection on the complex plane's real axis of a vector with magnitude $|F_{jk}| \sqrt{S_{yy,jj} S_{yy,kk}}$ scaled by $\sqrt{\gamma_{jk}^2}$ and with phase $\phi_{jk} - \theta_{jk}$. Being the coherence a real number between 0 and 1, the multiplication by its square root always scales down these vectors, represented in Figure 3 by the dash-dot arrows. The standard method suggests the

maximum possible reduction from the positive fixed term, since all the coherence are unitary and all the cosines are forced to have values of -1. Consequently, all the (unscaled) vectors are forced to lay on the negative real axis. This operation is accomplished by assigning the phases according to the Minimum Drives Condition (13a). In the proposed procedure, this is performed just to $\ell - 1$ vectors (i.e. elements of the reference matrix), that will contribute to reduce the drive traces. The phase of the remaining vectors are calculated from the ones set and thus these vectors projected to the real axis of the complex plane. Depending on the value of the resulting phase angle, they can contribute or not to the drive trace's reduction. It is worth to notice that, increasing the drive traces with respect to the one obtained from the standard method, is a direct consequence of the resulting reference matrix being positive semi-definite. A negative definite matrix can have a reduced traces due to the effect of negative eigenvalues (potentially, in the standard method, nothing stymies the drive traces to be also negative, as shown in Figure 3).

In order to guarantee the biggest trace reduction, the $\ell - 1$ chosen phases can be defined as the one corresponding with the vectors with biggest amplitude $|F_{jk}| \sqrt{S_{yy,jj} S_{yy,kk}}$.

It is fundamental to notice that the only information needed for this target definition method is the System Identification, anyhow required for the vibration control algorithm, and the PSD profiles, representing the test specifications. The target definition process can therefore be fully automated. Furthermore, the generated targets incorporate information coming from the system identification, that could result in exciting the system in agreement with its dynamic behavior.

Extending the work proposed in [29] to meet the minimum drives requirements, the proposed target generation procedure will be addressed as Minimum (Maximum) Drives Method and the generated targets as Minimum (Maximum) Drives Targets.

4. Test Cases

The Minimum (Maximum) Drives Method is tested with different actuation systems with two, three and six drives, in order to show the general applicability of the algorithm. In order to avoid possible energy sinks associated with the pseudo-inversion, just *square* well-conditioned configurations are considered with realizable PSDs [20]. For the control case with two drive signals, the so-called FRF Box is used. This hardware is able to mimic a dynamic MIMO system (up to four inputs, four outputs and four modes) and has tunable modal parameters such as natural frequencies, mode shapes, damping ratios and participation factors. For the case with three drives, the electromechanical three-axial shaker Dongling 3ES-10-HF-500 at the University of Ferrara is used. Finally, six drives are used to control the servo-hydraulic six-axis shaker of the KULeuven, the TEAM Cube^{TM}. As data acquisition system and vibration controller, a Siemens LMS SCADAS Mobile SCM205V with different input modules is used, driven by Simcenter LMS Test.Lab Multi-Axis Random Control.

Typically, for safety reasons, in a MIMO random control test the full level test is gradually achieved in sequential steps (here -6dB, -3dB and 0dB). All the results shown are for *normal end* tests, meaning that the full level (0 dB) has been successfully run for 1 min (within the abort limits). The results in terms of control SDM are just shown for the tests run with the Minimum Drives Target. These results are illustrated in a matrix subplot fashion. The subplots on the diagonal show the reference profiles and the PSDs achieved at the normal end, together with the abort and alarm thresholds; in the upper and lower triangular parts of the plot the amplitude (in g^2/Hz) and phases (in degrees) of the upper triangular CSDs are reported, respectively. Since the matrices are positive semi-definite and therefore hermitian, the subplots are also representative for the lower triangular CSDs (complex conjugates). It is fundamental to notice that for the same test setup, different tests are run with the same PSD profiles, considered as test specifications, and different CSDs, coming from the application of the Minimum Drives Method and also with common choices of coherence and phases between control channels.

To show the advantage of the developed procedure, the comparison with other choices for the CSDs is shown in terms of

- predicted drives rms from a system verification run prior to the test (to check the tests levels). These values are simply the rms (over the selected bandwidth) calculated from the drive PSDs returned by equation 4.
- Drive traces, to show the narrow band drive traces reduction.

- In addition to the drives trace, its RMS is also highlighted, as a global indicator for the drives' power reduction. During the test narrowband unpredictable differences could arise due to the several reason, such as the randomness of the process, the on-line control action that tunes the drives to match the target and/or system's non-linearities.

4.1. Two-Drives Two-Controls Electromechanical system

The first test case is the FRF-BOX, illustrated in Figure 4.

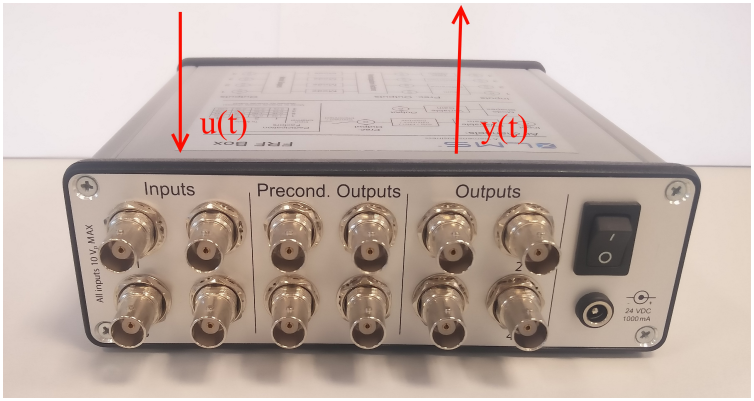

Figure 4: FRF Box. The system has tunable modal parameters.

The system's Inputs and Outputs are connected with the Siemens LMS SCADAS SCM205V (with vibration control capabilities). The simple case of two drives and two control channels has been considered, but the same conclusions have been found with three and four controls (and drives). The hardware is tuned in order to have three modes in the frequency range [50 1000] Hz at 160, 400 and 630 Hz with 1% of damping. The system's FRFs are illustrated in Figure 5. The resolution is set to 1.5625 Hz. The PSDs, fixed for the tests run, have a simple "haystack" shape with the breakpoints reported in Table 1, corresponding to overall levels of 0.403 g_{RMS}.

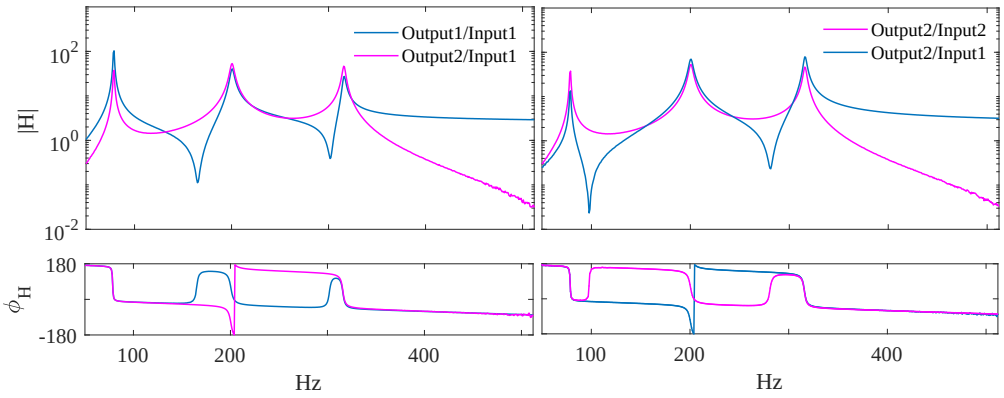

Figure 5: FRF matrix of the system tuned on the FRF Box. FRF amplitude in mV/V, phase angles in degrees.

Figure 6 shows the predicted drive levels from the pre-test System Verification. The different bars correspond to different choices in defining the CSDs. In the figure, the threshold for the overload of the data acquisition DAC is also reported. The figure shows the advantage, in terms of required drives power of adopting the Minimum Drives Method to set the CSD between the two controls. For example, the common choice of setting uncoherent controls needs more than twice the total power that the power needed using the developed method. Figure 6 also illustrates the power

frequency in Hz	PSD in g^2/Hz
0.5	0.01e-2
400	0.02e-2
600	0.02e-2
1024	0.01e-2

Table 1: breakpoints of the "haystack" profile used for the tests performed with the FRF Box.

reduction of the single drives. This allows to perform, with the same PSD profiles, a 0.8 g_{RMS}test that is impossible to reach in case low coherence is set between the responses: the Output 2 DAC overload limits the maximum test levels to 0.5 g_{RMS}. Figure 7 reports the narrowband control results for the test performed with the CSD set with the Minimum Drives Method. The step in the phase profile between 300 and 600 Hz reflects the system identification information embedded in the target. At 0 dB on the PSDs no spectral lines overcome the abort threshold and less then five spectral lines the alarm ones. The test has been successfully brought to the normal end. The resulting drive traces are finally compared with the ones resulting from other choices of coherence and phases in Figure 8. The Minimum Drives Method and the Maximum Drives Method return extreme drive traces in terms of RMS and narrowband results.

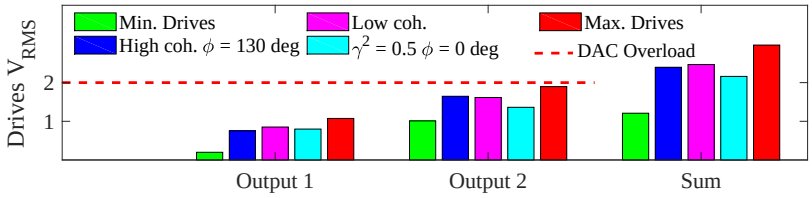

Figure 6: predicted drives and their sum, for the tests performed with the FRF Box.

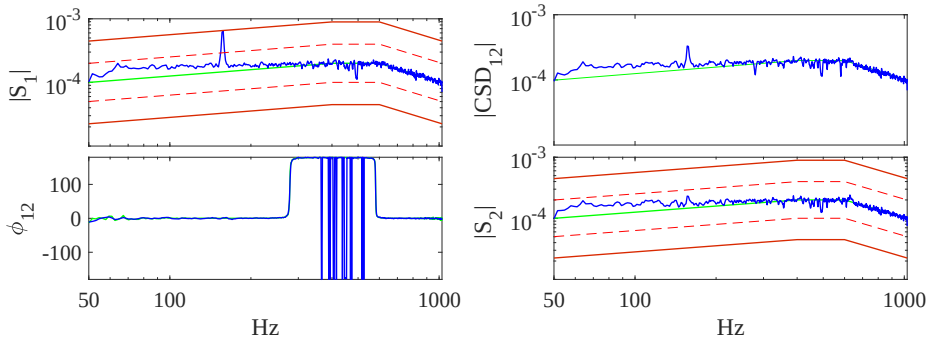

Figure 7: MIMO random control results (solid blue curve) for the test performed with the FRF Box by setting the target (solid green curve) with the Minimum Drives Method. PSDs and CSD's amplitude in g^2/Hz, phase angle in degrees. The solid red and dashed orange lines are the abort and alarm thresholds, respectively.

4.2. Three-Drives Three-Controls Test Cases

A simultaneous three-axial excitation is achieved using the electrodynamic tri-axial shaker of the University of Ferrara, shown in Figure 9.

This advanced actuation system is an assembly of three independent electrodynamic shakers, connected via a patented coupling hydrostatic bearing. The head expander is a squared 0.5 m plate with blunt corners and a total mass of 14 Kg. Two different series of tests are performed. First, the bare head expander (HE) is tested for the maximum allowed bandwidth. Subsequently, an automotive component is tested in a single simultaneous three-axial test to match the single axis specifications (longitudinal, lateral and vertical) in a simultaneous three-axial test.

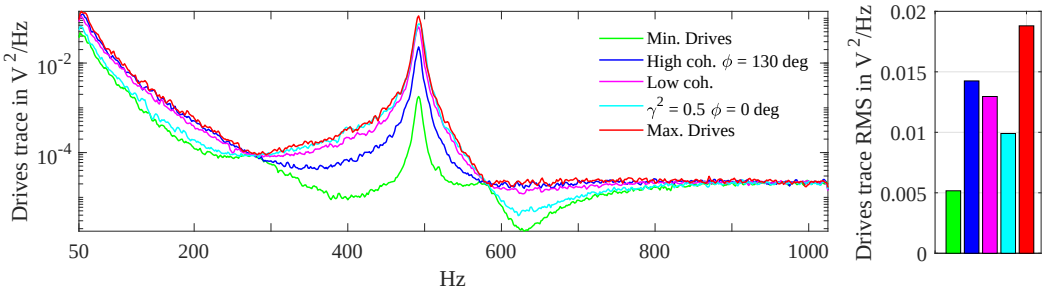

Figure 8: drive traces for the tests performed with the FRF Box.

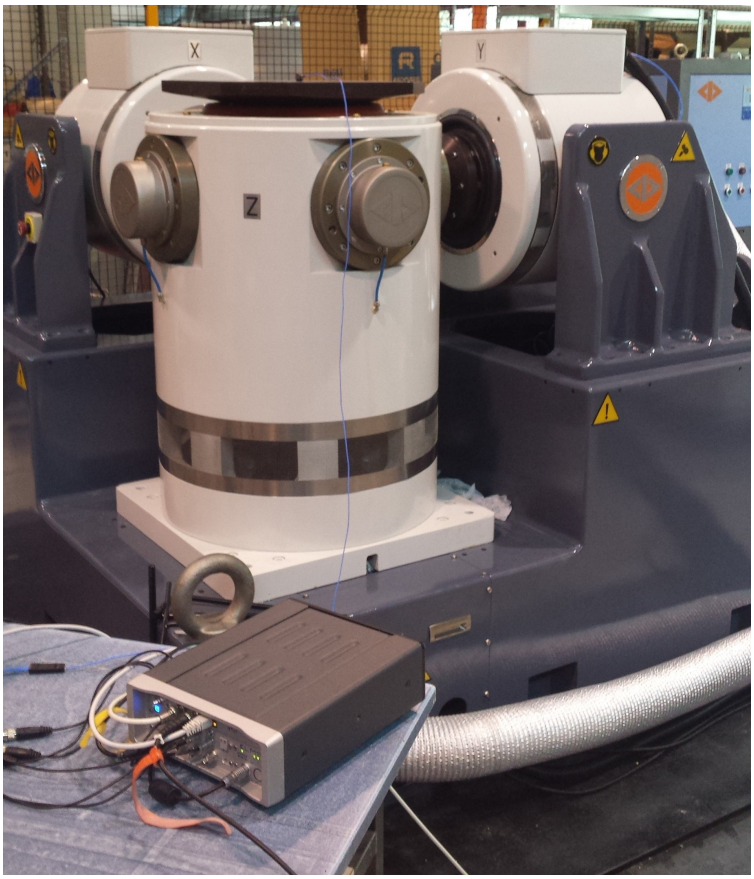

Figure 9: the Dongling 3ES-10-HF-500 three-axial shaker at the University of Ferrara.

Bare head expander. The HE is tested in the full frequency range allowed by the shaker's manufacturer ([10 – 2000] Hz) with the test configuration shown in Figure 10a and a frequency resolution of 1.5625 Hz. The control channels are the X, Y and Z axis of the accelerometer C1. The bandwidth pushes the limits of the shaker system and is well-above typical vibration control applications. Therefore, to get meaningful PSDs to be set as diagonal elements for the MIMO random control test, an open-loop pre-test is run with uncorrelated drives (pseudo random signals with a random phase randomization [33]). The X, Y and Z response RMS levels are 1.29, 1.25 and 1.45 g_{RMS}, respectively.

Figure 11 shows the predicted drives V_{RMS} and their sum for different target definition strategies. The figure allows to make some important considerations, already verified for the two-control two-drives case. Low coherence between responses does not necessarily mean low power, as shown via the equation (13a). The phase information set between

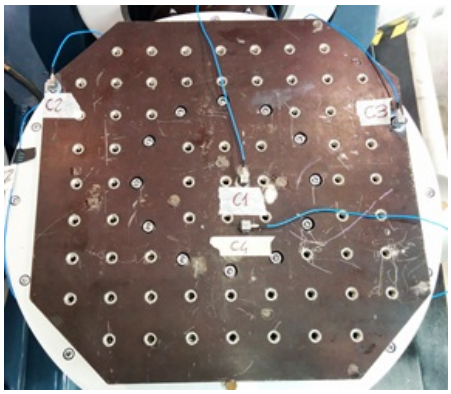

(a) bare head expander test configuration.

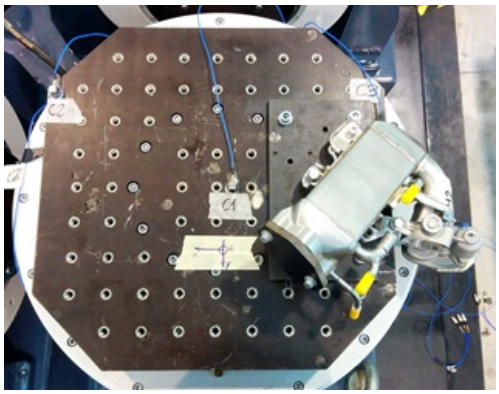

(b) test configuration with the EGR valve mounted on the head expander, top view.

(c) test configuration with the EGR valve mounted on the head expander, side view.

(d) test configuration with the EGR valve mounted on the head expander, front view.

Figure 10: test configuration for the tests performed with the three-axial shaker at the University of Ferrara.

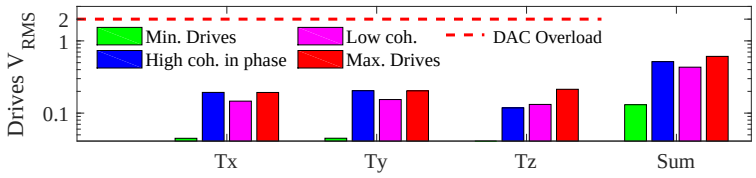

Figure 11: predicted drives and their sum, for the tests performed on the bare head expander with reference PSDs from an open loop pre-test.

the control channels is playing a major role. Choosing the phases with the Minimum Drives Method returns minimum predicted drives power, compared to the other choices.

Also for this test it is relevant to notice that the method shows a reduction of the single drives V_{RMS}. In case the test levels need to be increased, the method provides the biggest scaling factor. In case the same test levels are kept, choosing the CSDs with the Minimum Drives Method preserves the shakers and the amplifiers, subjected to lower voltages.

The control results for the normal end test with the target set with the Minimum Drives Method are shown in Figure 12 and the resulting drive traces are reported in Figure 13. As for the two controls case, the drive traces of the tests run by setting the CSDs with the Minimum and the Maximum Drives Method limit the drive traces returned by other phase and coherence selections.

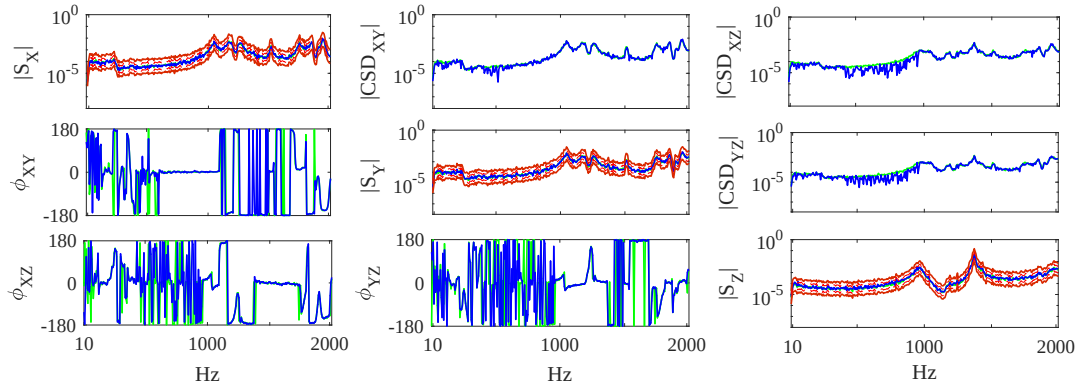

Figure 12: MIMO random control results (solid blue curve) for the test performed on the bare head expander of the three-axial shaker by setting the target (solid green curve) with the Minimum Drives Method. PSDs (diagonal subplots) and CSDs amplitudes (upper triangular subplots) in g^2/Hz, phase angles (lower triangular subplots) in degrees. The solid red and dashed orange lines are the abort and alarm thresholds, respectively.

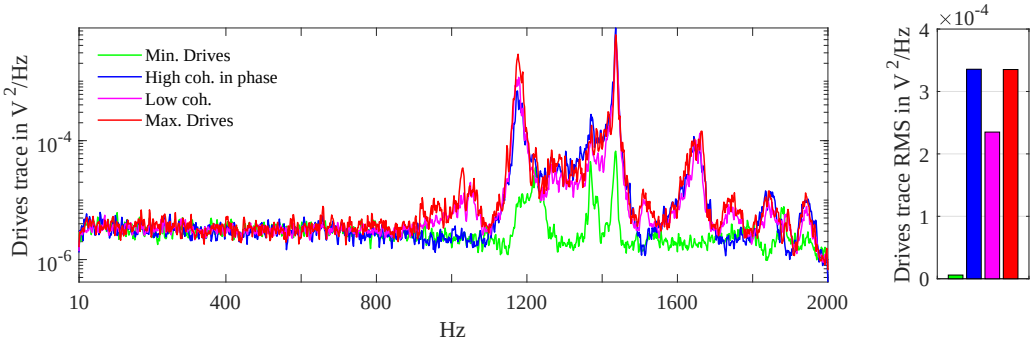

Figure 13: drive traces for the tests performed on the bare head expander with reference PSDs from an open loop test.

Automotive test article: Exhaust Gas Recirculation (EGR) valve. The successful tests motivated to use the Minimum Drives Method on an automotive OEM component to be tested to random vibration in the three different directions. The test specification are defined in terms of PSDs only, inherited from single axis test standard practices. The automotive component tested is an Exhaust Gas Recirculation (EGR) valve, used to reduce the internal combustion engines emissions. The test configuration is shown in the Figures 10b, 10c and 10d. For these tests, the same control channels adopted for the bare head expander test case are used. The PSD shapes come from single axis test specifications. They are defined in the frequency range [10 – 500] Hz, with a frequency resolution of 1.5625 Hz.

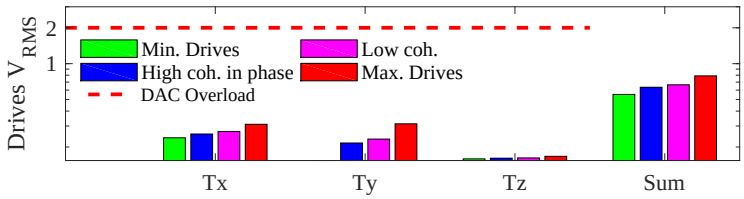

Figure 14: predicted drives and their sum, for the tests with the EGR valve mounted on the head expander.

The predicted drive voltages are illustrated in Figure 14 and show again the drives reduction obtained by the method. In this application the advantage in terms of voltage's reduction is evident but less significant compared to the previous test case. This is due to the reduced bandwidth, limited to a region where the cross-coupling between orthogonal axes is small and therefore the reference matrix's CSDs influence on the drives power reduces consequently.

Figure 15 shows the narrowband results of the MIMO random control process, with the response SDM perfectly controlled to achieve the Minimum Drives Target. The difference in the narrowband drive traces at the normal end can be seen in Figure 16, plotted in linear scale. The Minimum Drives Method shows a non negligible drives trace reduction. In the figure the theoretical Minimum (Maximum) drives trace are also reported. These traces are calculated substituting in equation (4) the response SDM with the target obtained applying the developed method and the system's FRF matrix with the one obtained from the system identification. The only region with an unexpected behaviors is a narrow band around 300 Hz, probably due to the control action performed to try to control the system's non-linearities. The adaptive feature of the Siemens LMS Multi-Axis Random Control can cope with system non-linearities, as shown in the good control results of Figure 15. On the contrary, the assumptions made to derive the Minimum Drives Target will be no longer valid and the effects of the drives correction could be unpredictable.

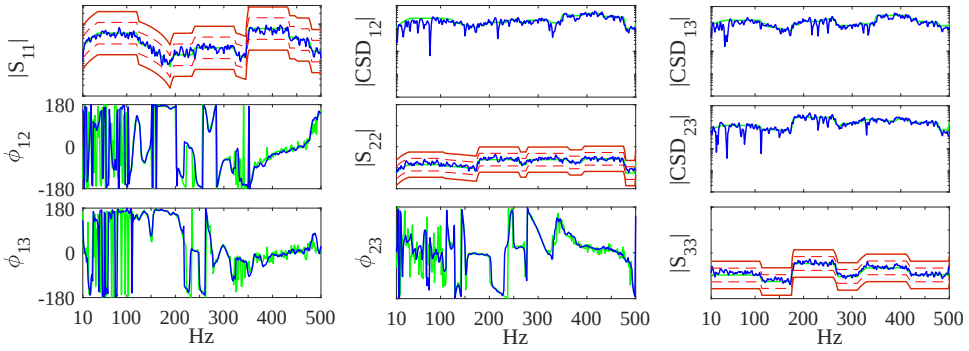

Figure 15: MIMO random control results (solid blue curves) for the test performed with the EGR valve mounted on the bare head expander of the three-axial shaker by setting the target (solid green curve) with the Minimum Drives Method. PSDs (diagonal subplots) and CSDs amplitudes (upper triangular subplots) in g^2/Hz, phase angles (lower triangular subplots) in degrees. The solid red and dashed orange lines are the abort and alarm thresholds, respectively.

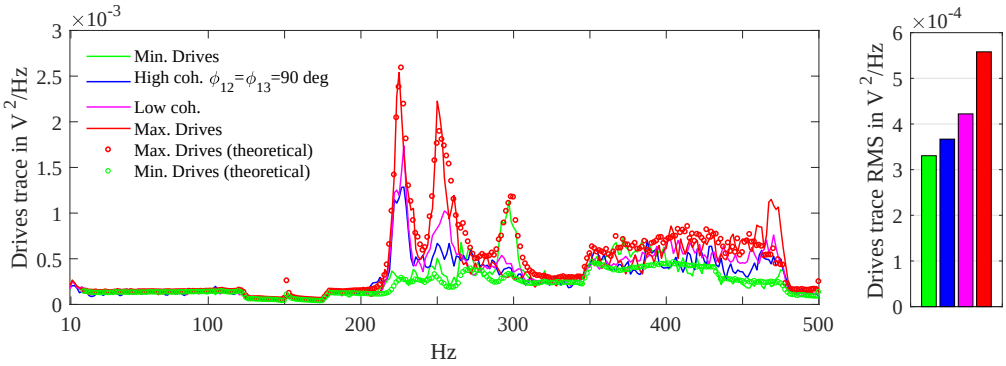

Figure 16: drive traces for the tests performed with the EGR valve mounted on the head expander.

4.3. Six-Drives Six-Controls Test Case

A full 6-DOFs motion can be provided by using the six-axis shaking system at the MECH lab of KU Leuven (Leuven, Belgium), the Team Cube™shown in Figure 17a and described in [34] and [35]. This state-of-the-art actuation is provided by three pairs of servo-hydraulic actuators in modal control: the six drives are therefore the three shaker's translations and the three rotations (Tx, Ty, Tz, Roll, Pitch and Yaw). In order to fully capture and control the shaker's motion, it is fundamental to adequately choose the sensors locations. The configuration chosen for the setup is illustrated in Figure 17b. Even though successful experiments have been performed loading the shaker with an automotive component, this section presents a series of tests on the empty shaker in the frequency range [18.75 – 150] Hz with a resolution of 1.5625 Hz.

(a) The TEAM Cube at the KU Leuven MECH lab.

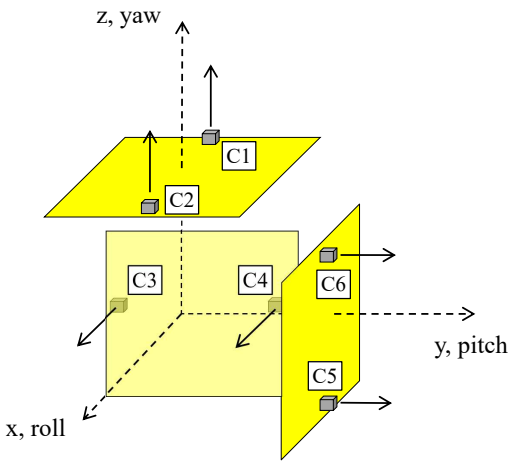

(b) Test configuration used with the Cube.

Figure 17: test configuration for the tests performed with the six-axis shaker at the KU Leuven, the TEAM Cube™.

frequency in Hz	PSD in g^2/Hz
18	3.34e-6
80	6.68e-5
150	6.68e-5

Table 2: breakpoints profiles used for the tests with the Cube™.

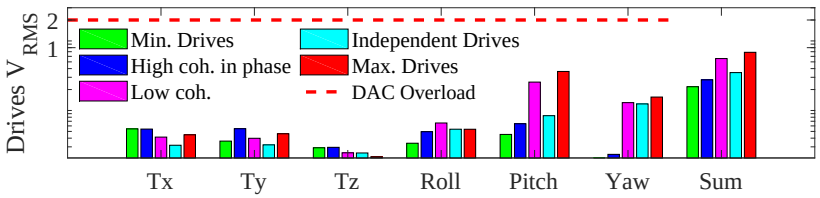

Figure 18: predicted drives and their sum for the tests performed on the Cube™.

The same PSD profile, reported in Table 2, is used for all the control channels. Different CSDs are set for the different experiments. It is understandable that, in case of six controls, even just setting a positive semi-definite target can be challenging, because a different reference matrix is defined per spectral line and the sizes of this matrix increase quadratically with the number of controls. Some typical solutions have been compared to the Minimum Drives Method. Particularly, the method has been compared with the method of the *Independent Drives*. The basic idea of the Independent Drives method is to try to find a set of uncorrelated inputs able to reproduce the desired control PSDs. The method is described in details in the Annex E of reference [2] as possible solution for minimizing the drives power, but is unfortunately not always able to guarantee a positive semi-definite reference matrix with the specified PSDs. As discussed for the test cases in the previous subsections, the Minimum Drives Method shows already in the pre-test system verification its advantages in terms of total drives power and the possibility of increasing the test levels. From Figure 18 it is possible to see that using the Minimum Drives Method (green bars) to set the CSDs between pairs of control channels would allow an up-scaling of the response levels up to 3 g_{RMS} before the Tx DAC

overloads. With the Independent Drives method (cyan bars), the Yaw DAC overload would limit the response levels up-scaling to only 1.4 g_{RMS}. Likewise, the Pitch DAC overload would limit the increase in response levels to 2.4 g_{RMS}, in case high coherent in phase responses are set between pairs of control channels (blue bars. For this application, the second best option in terms of total power reduction).

Figure 19 shows the control results obtained by setting the target with Minimum Drives Method. Comparable results were obtained with the other proposed methodologies. The resulting drive traces are finally shown in Figure 20. As predicted, globally the Minimum Drives Method shows the best total drives power reduction. Setting fully coherent and in phase response returns comparable results; however this is not a systematic result, as emphasized by Figure 16. Regarding the narrowband performances illustrated in Figure 20, a first conclusion would be that choosing fully coherent and in phase responses would return a drive power smaller than the one reached with the Minimum Drives Method. However for this specific case the two methods return comparable results in terms of drives power reduction and the narrowband subtle differences between the two methods are possibly due to the randomness of the control process.

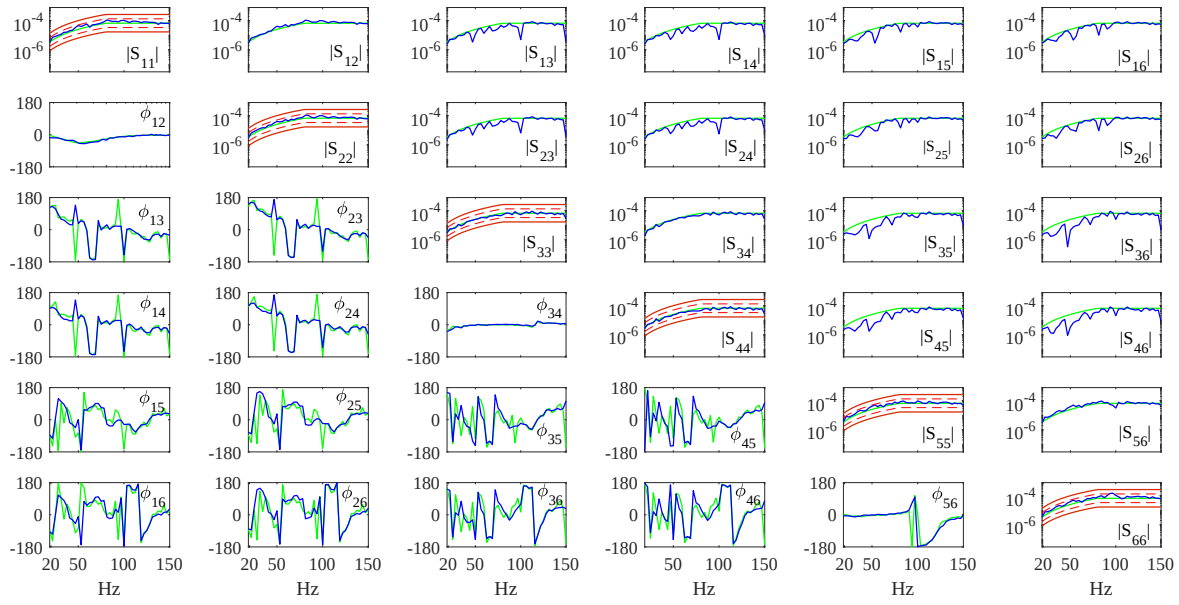

Figure 19: MIMO random control results (solid blue curves) for the test performed with the Cube^{TM}by setting the target (solid green curve) with the Minimum Drives Method. PSDs (diagonal subplots) and CSDs amplitudes (upper triangular subplots) in g^2/Hz, phase angles (lower triangular subplots) in degrees. The solid red and dashed orange lines are the abort and alarm thresholds, respectively.

5. Conclusions

This paper proposes the Minimum (Maximum) Drives Method as innovative fully automatic target definition procedure for MIMO random control tests. The method can be adopted in cases where the set of operational measurements is missing and/or test specifications are provided in terms of PSDs only. With the developed procedure it is possible to generate the missing CSDs in such a way that (i) the reference matrix is positive semi-definite in the whole test bandwidth and (ii) the drives power needed to reach the test specifications (the PSDs) is systematically reduced with respect to other possible state-of-the-art solutions. These features open the possibility to candidate the proposed methodology as attractive solution to the problem of meeting *the minimum drives criteria* and therefore to be included in the current standard practice for multi-axial testing.

The requirement of acceptable narrowband control performance is fulfilled, incorporating information about the system dynamics directly in the target (without additional measurement effort). Compared to standard choices or

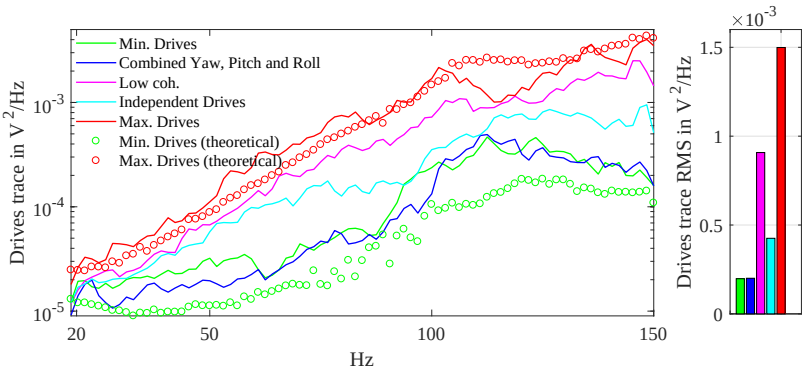

Figure 20: drive traces for the tests performed with the Cube^{TM}.

methods currently used to fill in the CSDs, the added value of reducing the total drives power is undoubtedly advantageous: for fixed test response levels, it guarantees that the delicate and expensive excitation hardware (shakers and amplifiers) is driven with reduced voltages. In case the test levels need to be increased, the proposed solution would allows a maximum scale factor. These advantages have been shown through a series of tests with different actuation systems (electronic, electrodynamic, servo-hydraulic shaker), number of drives (two, three and six drives) and number of control channels (two, three and six).

The possibility of minimizing/maximizing the drives power without modifying the PSD requirements is an attractive feature: further research can aim to assess the influence of the developed multi-axis random target definition procedure on the fatigue life of the article to be tested.

Acknowledgements

The authors would like to thank the PMA division of the Department of Mechanical Engineering of KU Leuven for using their six-axis shaking table. The financial support of VLAIO is greatefully acknowledged (research grant ADVENT: ADvanced Vibration ENvironmental Testing).

References

[1] United States Department of Defense, Method 514.6: Vibrations, 2008. United States Military Standard 810G.
[2] United States Department of Defense, Method 527.1: Multi-Exciter Tests, 2014. United States Military Standard 810G.
[3] M. Mršnik, J. Slavič, M. Boltežar, Multi-Axial Vibration Fatigue - A Theoretical and Experimental Comparison, Mechanical Systems and Signal Processing 76-77 (2016) 409–23.
[4] M. Ernst, E. Habtour, D. Abhijit, M. Polhand, M. Robeson, M. Paulus, Comparison of Electronic Component Durability Under Uniaxial and Multiaxial Random Vibrations, Journal of Electronic Packaging 137 (2015) 165–80.
[5] D. Gregory, F. Bitsie, D. O. Smallwood, Comparison of the response of a Simple Structure to Single Axis and Multiple Axis Random Vibration Inputs, in proc. of the 79th Shock and Vibration Symposium (2008).
[6] Y. Soucy, A. Côté, Reduction of Overtesting During Vibration Tests of Space Hardware, Canadian Aeronautics and Space Journal 48 (2002) 77–86.
[7] M. A. Underwood, Multi-exciter Testing Applications: Theory and Practice, in proc. of the Institute of Environmental Sciences and Technology (2002).
[8] D. O. Smallwood, Multiple Shaker Random Vibration Control - An Update, Technical Report, Sandia National Laboratories (1999).
[9] B. Peeters, J. Debille, Multiple-input-multiple-output random vibration control: theory and practice, in proc. of the International Conference on Noise and Vibration Engineering (2002).
[10] M. A. Underwood, Multi-shaker control: a review of the evolving state-of-the-art, in proc. of the Institute of Environmental Sciences and Technology (2016).
[11] D. O. Smallwood, A Random Vibration Control System for Testing a Single Test Item with Multiple Inputs, Technical Report, Sandia National Laboratories (1982).
[12] M. A. Underwood, Applications of Digital Computers in A. G. Piersol, Shock and Vibration Handbook, Mc. Graw Hill, New York, 2001, pp. 27.1-27.36.
[13] M. A. Underwood, Adaptive control method for multiexciter sine tests, United States Patent, nr. 5299459 (1994).
[14] M. A. Underwood, T. Keller, Recent system developments for multi-actuator vibration control Sound and Vibration 35 (2001) 16–3.

[15] M. A. Underwood, T. Keller, 8 Actuator System provides 1 DOF to 6 DOF controlled Satellite Qualification Testing up to 100 Hz, in proc. of the 28th Aerospace Testing Seminar (2014).
[16] M. Appolloni, R. B. Dacal, A. Cozzani, R. Knockaert, B. Thoen, Multi-Degrees-Of-Freedom vibration platform with MIMO Controller fo future spacecraft testing: and application case for virtual shaker testing,in proc. of the 29th Aerospace Testing Seminar (2015).
[17] P. M. Daborn, P. R. Ind, D. J. Ewins, Next-Generation Random Vibration Tests, in proc. of the 32nd IMAC Conference. 8 (2014).
[18] C. Roberts, D. J. Ewins, Multi-Axis Vibration Testing of an Aerodynamically Excited Structure, Journal of Vibration and Control, 1 (2016).
[19] P. K. Aggarwal, Dynamic (Vibration) Testing: Design Certification of Aerospace System, Technical Report, NASA Marshall Space Flight Center (2010).
[20] M. G. Alvarez Blanco, K. Janssens, F. Bianciardi, Experimental verification of projection algorithms and optimization routines for acoustic field uniformity enhancement in MIMO direct field acoustic control, in proc. of the International Conference on Noise and Vibration Engineering (2016) .
[21] M. A. Underwood, R. Ayres, T. Keller, Filling in the MIMO Matrix: part 1 - Performing Random Tests Using Field Data, Sound and Vibration 1 (2011) 5–14.
[22] P. Daborn, Scaling up the Impedance-Matched Multi-Axis Test (IMMAT) Technique, in proc. of the 35th IMAC Conference (2017).
[23] L. Jacobs, G. Tipton, K. Cross, N. Hunter, J. Harvie, G. Nelson, 6-DOF Shaker Test Input Derivation from Field Test, in proc. of the 35th IMAC Conference (2017).
[24] L. Jacobs, M. Ross, G. Tipton, K. Cross, N. Hunter, J. Harvie, G. Nelson, Experimental execution of 6-dof tests derived from field tests,in proc. of the 35th IMAC Conference (2017).
[25] P. M. Daborn, P. R. Ind, D. J. Ewins, Enhanced Ground-Based Vibration Testing for Aerodynamic Environments, Mechanical Systems and Signal Processing 49 (2014) 165–80.
[26] P. M. Daborn, Smarter dynamic testing of critical structures, Ph.D. Thesis, University of Bristol (2014).
[27] U. Musella, G. D'Elia, S. Manzato, B. Peeters, P. Guillaume, F. Marulo, Analyses of Target Definition Processes for MIMO Random Vibration Control Tests,in proc. of the 35th IMAC Conference (2017).
[28] U. Musella, G. D'Elia, B. Peeters, E. Mucchi, P. Guillaume, F. Marulo, in proc. of the 30th Aerospace Testing Seminar (2017).
[29] D. O. Smallwood, Multiple-Input Multiple-Output (MIMO) Linear Systems Extreme Inputs/Outputs, Shock and Vibration 14 (2007) 107.
[30] C. D. Meyer, Matrix analysis and applied linear algebra, Society for Industrial and Applied Mathematics, Philadelphia, 2000.
[31] J. Bendat, A. G. Piersol, Random data: analysis and measurement procedures, volume 729, John Wiley and sons, New York (NY), US, 2011.
[32] D. O. Smallwood, T. Paez, A Frequency-Domain Method for the Generation of Partially Coherent Normal Stationary Time-Domain Signals, Shock and Vibration 1 (1993) 45–53.
[33] B. Cornelis, A. Toso, W. Verpoest, B. Peeters, Improved MIMO FRF estimation and model updating for robust Time Waveform Replication on durability test rigs, in proc. of the International Conference on Noise and Vibration Engineering (2014).
[34] F. De Conink, Multi-axial road reproductions for non-linear road noise models, Ph.D. Thesis, KU Leuven (2007).
[35] B. Peeters, J. Debille, F. De Conink, Multi-Axial random vibration testing: a six-degrees-of freedom test case, in proc. of the International Conference on Noise and Vibration Engineering (2003).

Appendix A. Positive Semi-definite matrices in MIMO random vibration control

It can be demonstrated that the Spectral Density Matrices in multi-axial random control are positive semi-definite. By definition, a matrix $\mathbf{M}$ is positive semi-definite if and only if the scalar $\mathbf{z}^H\mathbf{M}\mathbf{z}$ is (semi-)positive for every non-zero column vector $\mathbf{z}$ of (generally complex) numbers. In random vibration control, the drives and the control signals are random signal (stationary and ergodic). Therefore for the random recordings $\mathbf{y}(t)$ it can be written

$$\mathbf{S_{yy}} = \lim_{N\to\infty}[\frac{1}{N}\sum_{i}^{N}(\mathbf{Y}_i\mathbf{Y}_i^H)] \tag{A.1}$$

where $\mathbf{Y}$ is the spectrum of the random recordings. By noticing that $\mathbf{YY}^H = \mathbf{YI_dY}^H$ and following the definition of positive semi-definite matrices, it is easy to see that the rank-1 matrix $\mathbf{YY}^H$ is positive semi-definite. Since the space of positive semi-definite matrices is convex, a summation of positive semi-definite matrices is still positive semi-definite. This is also true in case of scaling for a real semi-positive number $(1/N)$. Therefore the averaging process preserves the positive semi-definiteness of the matrix $\mathbf{YY}^H$ and $\mathbf{S_{yy}}$ is positive semi-definite.

There are some properties that have practical implication in Multi-Axial random vibration control. Considering the general set of signals $\mathbf{y}(t)$, saying that the Specral Density Matrix $\mathbf{S_{yy}}$ is positive semi-definite also means (necessary and sufficient conditions) that

(a) all the eigenvalues of $\mathbf{S_{yy}}$ are semi-positive;

(b) $\mathbf{S_{yy}}$ has a unique Cholesky Decomposition, meaning that it can be decomposed in the product of two triangular hermitian matrices, referred as the *Cholesky Factors*: $\mathbf{S_{yy}} = \mathbf{LL}^H$;

(c) the *Sylvester's Criterion* is respected, i.e. all the *Principal Minors* of $\mathbf{S_{yy}}$ have positive determinants. The Principal Minors are the square sub-matrices that share the diagonal with the full matrix and the first element.

Moreover, if $\mathbf{S_{yy}}$ is positive semi-definite then

(d) the trace of $\mathbf{S_{yy}}$ is real and semi-positive, being the matrix trace the sum of its eigenvalues;

(e) follows from (a) or (c) that the determinant of $\mathbf{S_{yy}}$ is real and semi-positive;

(f) also $\mathbf{S_{uu}} = \mathbf{Z}\mathbf{S_{yy}}\mathbf{Z}^H$ is positive semi-definite.

The property (b) is fundamental and allows the control algorithm to work on the Cholesky Decomposition of the target matrix (the approach proposed by Smallwood in [8] and [11]) or, following the property (f), of the drives matrix (as proposed by Underwood in [7]). Property (d) underlines that the method chosen for defining the target needs to guarantee that the trace of the matrix (and following property (f), of the drives matrix) needs to be positive.